Geochemical Perspectives Letters

Rhenium elemental and isotopic variations at magmatic temperatures

W. Wang, A.J. Dickson, M.A. Stow, M. Dellinger, K.W. Burton, P.S. Savage, R.G. Hilton, J. Prytulak

Supplementary Information

The Supplementary Information includes:

- Materials and Methods
- Tables S-1 to S-3
- Figure S-1
- Supplementary Information References

Materials and Methods

Hekla lavas

Hekla is a ridge shaped volcano in the South Iceland Volcanic Zone, and is, historically, one of the most active volcanoes on Iceland. It erupts a wide range of volcanic products with a range of SiO_2 from ~46 to 72 wt. %, covering basalts, basaltic andesites, andesites, dacites and rhyolites, from a cogenetic source (*e.g.*, Savage *et al.*, 2011).

It was generally considered that for the Hekla lavas: (1) basaltic magmas rise and trigger partial melting of the lower part of metabasaltic Icelandic crust to generate dacitic magma; (2) the basaltic magma and dacitic magma evolve by crystal fractionation, producing basaltic andesite and rhyolitic magma, respectively; (3) mixing of basaltic andesite and dacitic melts produces andesites (Sigmarsson *et al.*, 1992, 2022). However, it has recently been suggested that mineral compositional data are more consistent with the origin of the basaltic andesites and andesites by fractional crystallization (Geist *et al.*, 2021), arguing against the three-stage model.

This issue of the origin of the dacites—whether by fractional crystallisation of andesites or *via* partial melting of amphibolite—continues to be debated (*cf*. Sigmarsson, 2023; Geist *et al.*, 2023). However, the disagreement over the origin of the andesitic to silicic magma is not a concern for this study, as long as magmatic differentiation and/or remelting of cognate material link the production of the entire sequence of Hekla lavas. Furthermore, the origin of the basalt to basaltic andesites *via* fractional crystallisation is not contested, and it is this range where Re concentrations were high enough to determine Re isotopic compositions.

A previous study by Savage *et al.* (2011) on the same samples showed that silicon isotopic compositions correlate with SiO_2 content. Redox-sensitive isotope systems such as Fe and V also showed systematic isotopic fractionations during fractional crystallization (Schuessler *et al.*, 2009; Prytulak *et al.*, 2017). In contrast, for Li, Zn, Mo, Tl, K, N and Rb, no resolvable isotopic variation was found among the Hekla series of igneous rocks (Schuessler *et al.*, 2009; Chen *et al.*, 2013; Yang *et al.*, 2015; Prytulak *et al.*, 2017; Tuller-Ross *et al.*, 2019; Boocock *et al.*, 2023; Wang *et al.*, 2023).

Additional samples

Additional unrelated Icelandic samples are reported in this study. The sample RP80C-1 was dredged from 63° 49' N, 22° 39' W on the neovolcanic axis of the Reykjanes Ridge during the cruise CD80 of RRS Charles Darwin (Murton *et al.*, 2002); this sample has been previously analysed for strontium, lead and oxygen isotope ratios (Gee *et al.*, 1998; Thirlwall *et al.*, 2004, 2006). The samples BUR20-09 and RHY1-09 were collected from near Burfell, Iceland; their compositions have been widely reported in comparison to the Hekla lavas (*e.g.*, Yang *et al.*, 2015; Tuller-Ross *et al.*, 2019).

Three MORB samples from different mid-ocean ridge segments (one from the North Atlantic Ocean, one from the East Pacific Ocean, one from the Indian Ocean) were analysed in order to provide better constraints on Re isotopic composition of the upper mantle. Samples vary in chemical composition, with MgO ranging from ~6.8 to 7.8 wt. %. According to Marty and Zimmerman (1999), based on the measured K_2O/TiO_2 ratios, these MORB samples can be classified into two types: N-MORB (RDL DR30 and CYP 78 12-35; $K_2O/TiO_2 < 0.08$) and E-MORB (MD57 D'10-1; $K_2O/TiO_2 > 0.15$).

Rhenium concentration and isotope analysis

The Re concentrations of the samples were determined by isotope dilution following established methods (Birck *et al.*, 1997). Approximately 200 mg of sample powder was weighted into 7 mL PFA vials and ^{185}Re spike was added to each sample. Following equilibration, the digestion was achieved with 3:1 HF:HNO_3, and then 6 M HCl. Samples were subsequently taken up in 2 M HNO_3 and Re was extracted using 3-methyl-1-butanol (isoamylol) liquid-liquid extraction. The purified samples were re-dissolved in 0.4 mL 3 % HNO_3 containing 30 ppb W, and were measured on multi-collector inductively coupled plasma mass spectrometry (MC-ICP-MS; Neptune Plus) at Royal Holloway University of London. The Re concentration was calculated based on the known sample volume and the quantity of added spike.

The low Re concentration of these samples means that a mass of at least ~1 g (for the lowest Re concentration samples, up to ~10 g) is necessary for the precise determination of stable Re isotopes (δ^{187}Re). Aliquots of sample powders (~1 g) were initially digested in 3:1 concentrated HF and HNO_3 in 30 mL PFA vials at 120 °C for at least 48 h; note that digestion in multiple vials is typically needed for one sample. The samples were slowly evaporated to dryness and re-dissolved in aqua regia and heated at 120 °C to destroy fluorides, before being evaporated again. The samples were then taken up in 6 M HCl. A pressure digestion system (PicoTrace) was further utilised if undissolved material remained (Jerram *et al.*, 2020). Finally, samples were re-dissolved in 1 M HCl (20–40 mL for every ~1 g sample aliquot); care was taken to ensure complete dissolution.

Prior to the isotopic analysis, the Re was purified using a three-step column procedure, adapted from Dellinger *et al.* (2020) and Dickson *et al.* (2020). First, 2 mL AG1-X8 (200–400 mesh) anion exchange resin was loaded into polypropylene BioRad columns, and was cleaned with 30 mL 7.5 M HNO_3 and pre-conditioned with, respectively, 10 mL 4 M and 3 mL 1 M HCl. Samples were loaded onto the columns in 1 M HCl, with a further addition of 20 mL 1 M HCl and 4 mL 3 M HNO_3 to remove matrix elements and transition metals. Thereafter, Re was eluted with 15 mL 7.5 M HNO_3. Note that some samples were dissolved in large volume of 1 M HCl (up to 200 mL, considering multiple aliquots/vials). In this case, in order to reduce the loading time, it was advisable to use multiple polypropylene BioRad columns for one same sample at this step; the collected fractions were then combined before loaded onto the micro-column (as below).

In the second step, samples were evaporated to dryness, re-dissolved in 1 mL 1 M HCl, and loaded onto 200 µL anion resin in Teflon micro-columns. Matrix elements were eluted with the additions of 1.5 mL 1 M HCl and 0.4 mL 3 M HNO_3. Re was then eluted with 2 mL 7.5 M HNO_3. This second step was repeated

one more time to purify the Re from the residual matrix. Samples were refluxed in concentrated HNO_3 at 120 °C for at least 24 h after each column step to destroy resin-derived organic residues.

The stable Re isotopic composition of the samples was determined by MC-ICP-MS (Neptune Plus) at Royal Holloway University of London, using the same methods as described in Dickson *et al.* (2020). The instrument was fitted with 10^{13} Ω amplifiers and was running in wet plasma mode with standard wet-plasma sample cones and 'H' skimmer cones. Purified samples with concentrations of ~1 to 3 ppb Re were introduced using a quartz SIS spray chamber and signals from ^{184}W, ^{185}Re, ^{186}W, ^{187}Re, ^{189}Os and ^{190}Os were quantified. Each analytical sequence consisted of repeat analyses of the NIST3143 and NIST989 standard reference materials (SRM) with every three samples. Each measurement comprised a single block of 40 × 8.5 s integrations, preceded by 10 integrations of 3 % HNO_3 blank solution.

The instrumental mass bias was corrected by doping each sample to 30 ppb tungsten (W) with NIST SRM 3163, and by using an exponential law with the measured $^{186}W/^{184}W$ (Miller *et al.*, 2015; Dellinger *et al.*, 2020; Dickson *et al.*, 2020). This method assumed that W and Re share the same degree of mass bias in the instrument (Poirier and Doucelance, 2009). The Re/W ratios for the measured samples were within ±10 % of that for the bracketing standards. The final Re isotope value of the samples was reported in delta notation relative to the NIST SRM 3143 and expressed as:

$$\delta^{187}Re\ (‰) = [(^{187}Re/^{185}Re)_{sample}/(^{187}Re/^{185}Re)_{NIST3143} - 1] \times 1000\ . \qquad (S\text{-}1)$$

The overall procedure blank for the Re isotope analysis (digestion and purification) was below 10 pg Re, which was <2 % of the total Re analysed. Rhenium isotope fractionation can occur during column chromatography (Miller *et al.*, 2009; Liu *et al.*, 2017). The recovery of Re in this study was >60 % for all samples. As shown in Miller *et al.* (2009), when eluting the Re using 4 M HNO_3, a >60 % recovery will likely lead to <0.05 ‰ fractionation; this is smaller than the analytical error presented in this study. Furthermore, as discussed in Dellinger *et al.* (2020) and Dickson *et al.* (2020), column fractionation effects are likely negligible when eluting Re with higher molarity of HNO_3; consistent with Dellinger *et al.* (2020) and Dickson *et al.* (2020), in this study the elution was done with 7.5 M HNO_3, which should render any measurable fractionation minimal.

The precision and accuracy of the above methods were further validated through the analysis of (1) NIST 989 and ICP Re standard solutions, and (2) inter-comparison samples, including BHVO-2, BIR-1, BCR-2 and MAG-1; the results are summarised in Table S-1.

Modelling the evolution of Re and δ^{187}Re

We aim to produce an internally consistent model for Re-MgO during magma differentiation, and undertook the same modelling approach as described Prytulak *et al.* (2017). The fractionating assemblage at Hekla consists of olivine (and later orthopyroxene), plagioclase, clinopyroxene and titanomagnetite (Sigmarsson *et al.*, 1992; Geist *et al.*, 2021). We use the most primitive (highest Re concentration) lavas as a starting point, and the modelling was performed at 5 % intervals of melt remaining (F). The Re partition coefficients for orthopyroxene and clinopyroxene are taken as 0.013 and 0.2, respectively, based on Li (2014) and references therein. The Re partition coefficient for magnetite is adjusted so as to best fit the data, and is derived to be $D_{\mathrm{Re}}^{\mathrm{Mag}} \approx 50$. This is nevertheless consistent with the MELTS modelling results by Righter *et al.* (1998) for a sulfide-free system.

A Rayleigh fractionation model is applied to assess the extent of Re isotope fractionation during crystallisation:

$$\delta^{187}\mathrm{Re}_{\mathrm{melt}} = \delta^{187}\mathrm{Re}_{\mathrm{bulk}} + \Delta^{187}\mathrm{Re}_{\mathrm{min\text{-}melt}}\ln(F_{\mathrm{Re}}) \,, \qquad \text{(S-2)}$$

where F_{Re} is the fraction of Re remaining in the liquid. Changes in the abundance of perfectly incompatible elements have been used to estimate the fraction of melt remaining in evolving magmatic systems; here we choose Rubidium (Rb) for the calculation (Prytulak *et al.*, 2017). We assume 1.00005 as the bulk Re isotope fractionation factor during crystallisation of magnetite, based on theoretical modelling by Miller *et al.* (2015). On the other hand, if kinetic fractionation occurs during degassing of Re, then the Re isotope fractionation factor would possibly be as large as ~0.9959. The modelling results are illustrated in Figure 3.

Supplementary Tables

Table S-1 Re isotopic composition for standard solutions and method validation samples.

Sample	Measured values					Recommended values	
	Re (ng/g)	δ^{187}Re (‰)	2 s.d. (‰)	No. of measurements		Re (ng/g)	δ^{187}Re (‰)
Standard solutions							
NIST 989		**-0.28**	0.05	18			-0.29 ± 0.07 ‰ (Miller *et al.*, 2009), -0.28 ± 0.05 ‰ (Dellinger *et al.*, 2020), -0.27 ± 0.10 ‰ (Dickson *et al.*, 2020)
ICP Re		**-0.16**	0.11	15			-0.15 ± 0.07 ‰ to -0.19 ± 0.09 ‰ (Dickson *et al.*, 2020)
	Re (ng/g)	δ^{187}Re (‰)				Re (ng/g)	δ^{187}Re (‰)
		(1)	2 s.e.	*(2)*	2 s.e.		
Inter-comparison samples							
BHVO-2 (Hawaiian basalt)	0.55	-0.25	0.19			0.54 ng/g (Jochum *et al.*, 2016), 0.61 ng/g (Dellinger *et al.*, 2020)	-0.34 ± 0.06 ‰ (Dellinger *et al.*, 2020)
BHVO-2 (Hawaiian basalt) (*replicate*)		-0.42	0.12				
BIR-1 (Icelandic basalt)	0.64	-0.28	0.09	-0.28	0.10	0.65 ng/g (Jochum *et al.*, 2016), 0.70 ng/g (Dellinger *et al.*, 2020)	-0.34 ± 0.07 ‰ (Dellinger *et al.*, 2020)
BCR-2 (Columbia River Flood basalt)	11.0	-0.25	0.04	-0.26	0.10	12.6 ng/g (Jochum *et al.*, 2016), 11.6 ng/g (Dellinger *et al.*, 2020)	-0.29 ± 0.04 ‰ (Dellinger *et al.*, 2020)
BCR-2 (Columbia River Flood basalt) (*replicate*)		-0.35	0.07	-0.36	0.06		
MAG-1 (marine mud)	3.10	-0.36	0.09	-0.38	0.09	3.91 ng/g (Meisel and Moser, 2004), 3.65 ng/g (Dellinger *et al.*, 2020)	-0.28 ± 0.05 ‰ (Dellinger *et al.*, 2020)

2 s.d. = 2 times standard deviations of replicated analyses of the sample; 2 s.e. is the internal error of each individual MC-ICP-MS measurement and reflects the analytical uncertainty. Numbers *(1)* and *(2)* represent up to two repeat MC-ICP-MS measurements on the same sample solution.

Table S-2 All Re data presented in this study.

Sample	Re (ng/g)		δ^{187}Re (‰)						Description	Age
	Average	2 s.d.	*(1)*	2 s.e.	*(2)*	2 s.e.	Average	2 s.d.		
Hekla lavas										
HEK1-09	0.021	0.002							Dacite	2800 BP
HEK2-09	0.209	0.003	-0.22	0.11			**-0.22**	N.A.	Basaltic andesite	1970 AD
HEK3-09	0.206	0.004							Basaltic andesite	1970 AD
HEK4-09	1.372	0.006	-0.28	0.09	-0.33	0.10	**-0.30**	0.06	Basalt	1878 BP
HEK6-09	1.417	0.006	-0.28	0.10			**-0.28**	N.A.	Basalt	1913 AD
HEK7-09	1.317	0.006							Basalt	1878 AD
HEK8-09	0.187	0.005							Basaltic andesite	1970 AD
HEK9-09	1.234	0.007	-0.26	0.07	-0.31	0.06	**-0.28**	0.08	Basalt	1878 AD
HEK10-09	0.154	0.002	-0.33	0.14			**-0.33**	N.A.	Andesite	1947 AD
HEK11-09	0.117	0.003							Andesite	1947 AD
HEK12-09	1.246	0.005	-0.31	0.09	-0.33	0.08	**-0.32**	0.03	Basalt	1913 AD
HEK13-09	0.231	0.003							Basaltic andesite	1991 AD
HEK14-09	0.221	0.004	-0.22	0.12			**-0.22**	N.A.	Basaltic andesite	1991 AD
HEK16-09	0.165	0.004	-0.45	0.12			**-0.45**	N.A.	Basaltic andesite	1980 AD
HEK17-09	0.209	0.003							Basaltic andesite	1980 AD
HEK18-09	0.026	0.003							Dacite	2800 BP
HEK19-09	0.026	0.002							Dacite	2800 BP
HEK21-09	0.132	0.009							Basaltic andesite	1390 AD

Table S-2 continued

Sample	Re (ng/g)		δ^{187}Re (‰)						Description	Age
	Average	2 s.d.	*(1)*	2 s.e.	*(2)*	2 s.e.	Average	2 s.d.		
Other Icelandic										
RP80C-1	0.851	0.017	-0.30	0.11	-0.32	0.11	**-0.33**	0.08 (*n* = 5)	Basalt	8000–9000 BP
RP80C-1 (*replicate 1*)			-0.40	0.07	-0.33	0.06				
RP80C-1 (*replicate 2*)			-0.32	0.09						
BUR20-09	0.631	0.004	-0.40	0.10	-0.31	0.08	**-0.35**	0.13	Basalt	~1700 AD
RHY1-09	0.103	0.002							Dacite	Postglacial
Mid-ocean ridge basalts										
RDL DR30	0.781	0.015	-0.33	0.06			**-0.33**	N.A.	Atlantic Ocean (21° 82' N, 45° 22' W)	
CYP 78 12-35	1.431	0.029	-0.44	0.07			**-0.44**	N.A.	Pacific Ocean (20° 90' N, 109° 05' W)	
MD57 D'10-1	0.991	0.020	-0.43	0.08			**-0.43**	N.A.	Indian Ocean (06° 22' S, 68° 25' E)	

2 s.d. = 2 times standard deviations of repeat analyses of the sample; 2 s.e. is the internal error of each individual MC-ICP-MS measurement; N.A. = not available. Numbers *(1)* and *(2)* represent up to two repeat MC-ICP-MS measurements on the same sample solution.

In Figures 1 and 3, uncertainties on δ^{187}Re represent the 2 s.d. of repeat MC-ICP-MS measurements on the same sample (or 2 s.e. internal error if there was only one measurement), or the long-term reproducibility for the standard solution (ICP: 0.11 ‰; Table S-1), whichever is larger. Uncertainties on Re concentration represent the 2 s.d. of repeat measurements on the same sample; for the MORBs, a 2 % uncertainty is assigned as an estimate of the external reproducibility.

Table S-3 Ancillary data presented in this study.

Sample	SiO_2 (wt. %)	MgO (wt. %)	TiO_2 (wt. %)	S (µg/g)	Mo (µg/g)	V (µg/g)	Yb (µg/g)	Th (µg/g)	Rb (µg/g)
Hekla lavas									
HEK1-09	68.71	0.26	0.33	0	3.9	5	7.49	9.0	54.1
HEK2-09	53.92	2.86	2.01	31	2.6	50	6.48	3.7	24.8
HEK3-09	54.05	2.92	2.04	40	2.6	49	6.37	4.6	24.9
HEK4-09	46.97	5.53	4.42	123	1.4	319	3.73	2.1	12.1
HEK6-09	46.20	5.40	4.51	172	1.3	314	3.72	2.2	11.8
HEK7-09	46.64	5.57	4.31	124	1.4	309	3.69	2.7	12.7
HEK8-09	54.59	2.68	1.90	49	2.7	49	6.60	4.8	27.0
HEK9-09	47.01	5.30	4.53	122	1.5	317	4.14	2.3	12.3
HEK10-09	57.67	2.17	1.48	15	2.8	32	5.96	3.3	31.2
HEK11-09	58.09	2.16	1.47	6	2.7	30	5.98	5.3	31.2
HEK12-09	46.42	5.23	4.47	104	1.4	304	4.05	3.3	13.5
HEK13-09	53.90	2.98	2.12	57	2.5	66	6.25	4.5	23.8
HEK14-09	53.71	2.97	2.12	39	2.4	64	6.49	4.5	24.9
HEK16-09	54.81	2.74	1.96	42	2.6	53	6.61	4.7	25.7
HEK17-09	54.57	2.86	2.06	58	3.6	57	6.44	4.6	25.5
HEK18-09	68.41	0.25	0.31	2	3.9	2	7.49	9.2	53.2
HEK19-09	68.88	0.25	0.32	0	3.9	4	7.45	9.7	55.7
HEK21-09	55.64	2.58	1.77	26	2.7	34	6.74	4.9	28.6

Table S-3 continued

Sample	SiO_2 (wt. %)	MgO (wt. %)	TiO_2 (wt. %)	S (µg/g)	Mo (µg/g)	V (µg/g)	Yb (µg/g)	Th (µg/g)	Rb (µg/g)
Other Icelandic									
RP80C-1	N.A.	8.15	N.A.	N.A.	N.A.	N.A.	N.A.	N.A.	N.A.
BUR20-09	49.05	7.57	1.47	0	0.3	300	2.38	0.3	2.9
RHY1-09	68.53	0.54	0.43	6	6.0	16	5.81	18.2	111
Mid-ocean ridge basalts									
RDL DR30	51.25	7.01	1.75	1540	0.2	390	4.84	0.2	1.1
CYP 78 12-35	50.61	7.81	1.46	1198	0.2	296	3.36	0.2	1.4
MD57 D'10-1	50.69	6.84	1.68	1127	0.4	316	3.36	0.6	5.3

Ancillary data for the Hekla lavas and other Icelandic samples are from: Savage *et al.* (2011) (major elements), Prytulak *et al.* (2017) (trace elements), Thirlwall *et al.* (2006) (RP80C-1); ancillary data for the MORBs are partly from Gannoun *et al.* (2007).

Supplementary Figures

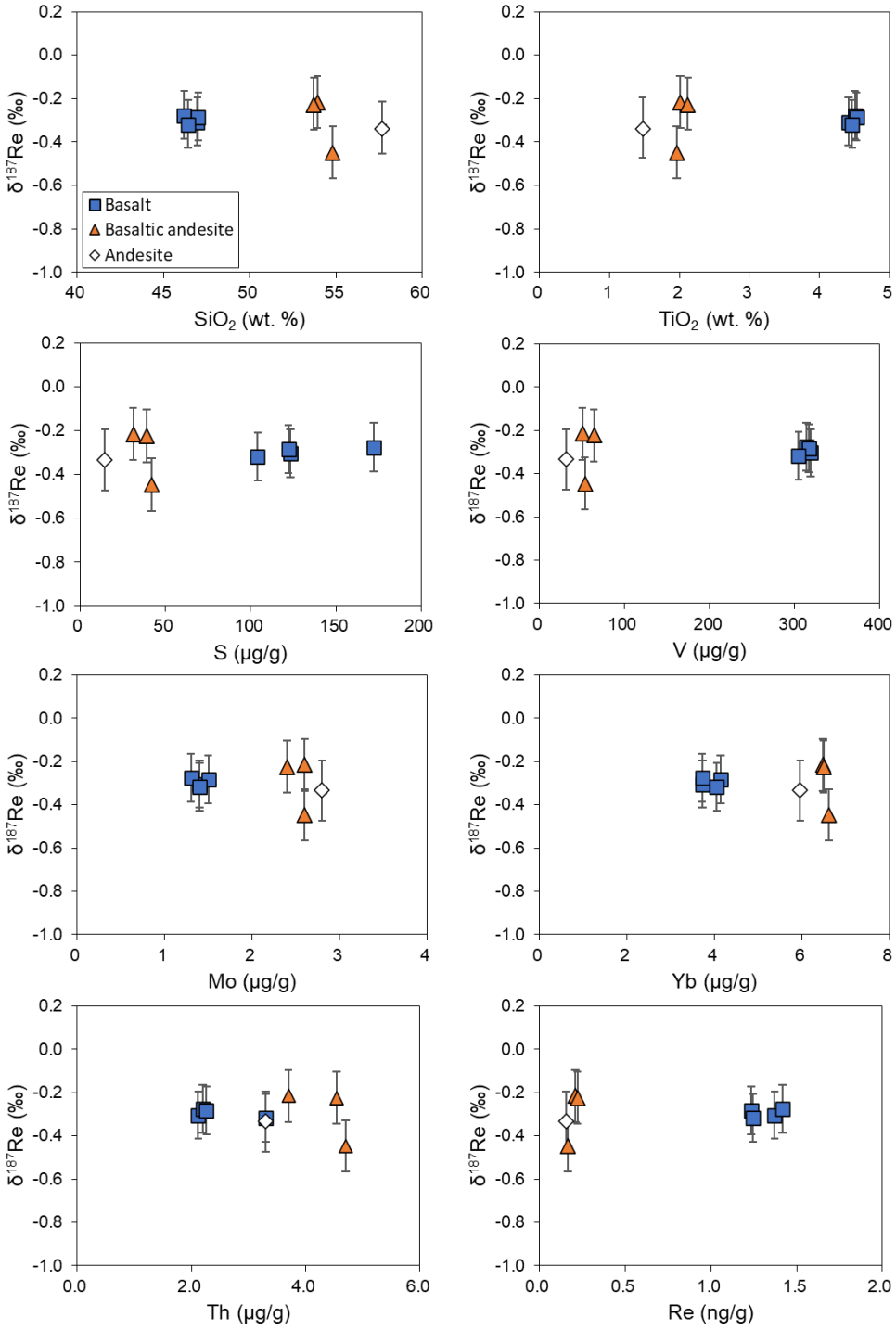

Figure S-1 Re isotope (δ^{187}Re) variations with SiO_2, TiO_2, S, V, Mo, Yb, Th, and Re concentrations in the Hekla lavas. Error bars on δ^{187}Re represent the 2 s.d. of repeat MC-ICP-MS measurements on the same sample (or 2 s.e. internal error if there was only one measurement), or the long-term reproducibility for the standard solution (ICP: 0.11 ‰), whichever is larger.

Supplementary Information References

Birck, J.L., Barman, M.R., Capmas, F. (1997) Re-Os Isotopic Measurements at the Femtomole Level in Natural Samples. *Geostandards Newsletter* 21, 19–27. https://doi.org/10.1111/j.1751-908X.1997.tb00528.x

Boocock, T.J., Mikhail, S., Boyce, A.J., Prytulak, J., Savage, P.S., Stüeken, E.E. (2023) A primary magmatic source of nitrogen to Earth's crust. *Nature Geoscience* 16, 521–526. https://doi.org/10.1038/s41561-023-01194-3

Chen, H., Savage, P.S., Teng, F.-Z., Helz, R.T., Moynier, F. (2013) Zinc isotope fractionation during magmatic differentiation and the isotopic composition of the bulk Earth. *Earth and Planetary Science Letters* 369–370, 34–42. https://doi.org/10.1016/j.epsl.2013.02.037

Dellinger, M., Hilton, R.G., Nowell, G.M. (2020) Measurements of rhenium isotopic composition in low-abundance samples. *Journal of Analytical Atomic Spectrometry* 35, 377–387. https://doi.org/10.1039/C9JA00288J

Dickson, A.J., Hsieh, Y.-T., Bryan, A. (2020) The rhenium isotope composition of Atlantic Ocean seawater. *Geochimica et Cosmochimica Acta* 287, 221–228. https://doi.org/10.1016/j.gca.2020.02.020

Gannoun, A., Burton, K.W., Parkinson, I.J., Alard, O., Schiano, P., Thomas, L.E. (2007) The scale and origin of the osmium isotope variations in mid-ocean ridge basalts. *Earth and Planetary Science Letters* 259, 541–556. https://doi.org/10.1016/j.epsl.2007.05.014

Gee, M.A.M., Thirlwall, M.F., Taylor, R.N., Lowry, D., Murton, B.J. (1998) Crustal Processes: Major Controls on Reykjanes Peninsula Lava Chemistry, SW Iceland. *Journal of Petrology* 39, 819–839. https://doi.org/10.1093/petroj/39.5.819

Geist, D., Harpp, K., Oswald, P., Wallace, P., Bindeman, I., Christensen, B. (2021) Hekla Revisited: Fractionation of a Magma Body at Historical Timescales. *Journal of Petrology* 62, egab001. https://doi.org/10.1093/petrology/egab001

Geist, D., Wallace, P., Harpp, K., Oswald, P. (2023) A discussion of: long or short silicic magma residence time beneath Hekla volcano, Iceland? *Contributions to Mineralogy and Petrology*, 178, 71. https://doi.org/10.1007/s00410-023-02049-1

Jerram, M., Bonnand, P., Kerr, A.C., Nisbet, E.G., Puchtel, I.S., Halliday, A.N. (2020) The δ^{53}Cr isotope composition of komatiite flows and implications for the composition of the bulk silicate Earth. *Chemical Geology* 551, 119761. https://doi.org/10.1016/j.chemgeo.2020.119761

Jochum, K.P., Weis, U., Schwager, B., Stoll, B., Wilson, S.A., Haug, G.H., Andreae, M.O., Enzweiler, J. (2016) Reference Values Following ISO Guidelines for Frequently Requested Rock Reference Materials. *Geostandards and Geoanalytical Research* 40, 333–350. https://doi.org/10.1111/j.1751-908X.2015.00392.x

Li, Y. (2014) Comparative geochemistry of rhenium in oxidized arc magmas and MORB and rhenium partitioning during magmatic differentiation. *Chemical Geology* 386, 101–114. https://doi.org/10.1016/j.chemgeo.2014.08.013

Liu, R., Hu, L., Humayun, M. (2017) Natural variations in the rhenium isotopic composition of meteorites. *Meteoritics & Planetary Science* 52, 479–492. https://doi.org/10.1111/maps.12803

Marty, B., Zimmermann, L. (1999) Volatiles (He, C, N, Ar) in mid-ocean ridge basalts: assesment of shallow-level fractionation and characterization of source composition. *Geochimica et Cosmochimica Acta* 63, 3619–3633. https://doi.org/10.1016/S0016-7037(99)00169-6

Meisel, T., Moser, J. (2004). Reference materials for geochemical PGE analysis: new analytical data for Ru, Rh, Pd, Os, Ir, Pt and Re by isotope dilution ICP-MS in 11 geological reference materials. *Chemical Geology* 208, 319–338. https://doi.org/10.1016/j.chemgeo.2004.04.019

Miller, C.A., Peucker-Ehrenbrink, B., Ball, L. (2009) Precise determination of rhenium isotope composition by multi-collector inductively-coupled plasma mass spectrometry. *Journal of Analytical Atomic Spectrometry* 24, 1069–1078. https://doi.org/10.1039/B818631F

Miller, C.A., Peucker-Ehrenbrink, B., Schauble, E.A. (2015) Theoretical modeling of rhenium isotope fractionation, natural variations across a black shale weathering profile, and potential as a paleoredox proxy. *Earth and Planetary Science Letters* 430, 339–348. https://doi.org/10.1016/j.epsl.2015.08.008

Murton, B.J., Taylor, R.N., Thirlwall, M.F. (2002) Plume–Ridge Interaction: a Geochemical Perspective from the Reykjanes Ridge. *Journal of Petrology* 43, 1987–2012. https://doi.org/10.1093/petrology/43.11.1987

Poirier, A., Doucelance, R. (2009) Effective Correction of Mass Bias for Rhenium Measurements by MC-ICP-MS. *Geostandards and Geoanalytical Research* 33, 195–204. https://doi.org/10.1111/j.1751-908X.2009.00017.x

Prytulak, J., Sossi, P.A., Halliday, A.N., Plank, T., Savage, P.S., Woodhead, J.D. (2017) Stable vanadium isotopes as a redox proxy in magmatic systems? *Geochemical Perspectives Letters* 3, 75–84. https://doi.org/10.7185/geochemlet.1708

Righter, K., Chesley, J.T., Geist, D., Ruiz, J. (1998) Behavior of Re during Magma Fractionation: an Example from Volcán Alcedo, Galápagos. *Journal of Petrology* 39, 785–795. https://doi.org/10.1093/petroj/39.4.785

Savage, P.S., Georg, R.B., Williams, H.M., Burton, K.W., Halliday, A.N. (2011) Silicon isotope fractionation during magmatic differentiation. *Geochimica et Cosmochimica Acta* 75, 6124–6139. https://doi.org/10.1016/j.gca.2011.07.043

Schuessler, J.A., Schoenberg, R., Sigmarsson, O. (2009) Iron and lithium isotope systematics of the Hekla volcano, Iceland — Evidence for Fe isotope fractionation during magma differentiation. *Chemical Geology* 258, 78–91. https://doi.org/10.1016/j.chemgeo.2008.06.021

Sigmarsson, O. (2023) Reply to comment on "Long or short silicic magma residence time beneath Hekla volcano, Iceland?" by Sigmarsson O, Bergþórsdóttir I A, Devidal J-L, Larsen G, Gannoun A. *Contributions to Mineralogy and Petrology*, 178, 72. https://doi.org/10.1007/s00410-023-02051-7

Sigmarsson, O., Condomines, M., Fourcade, S. (1992) A detailed Th, Sr and O isotope study of Hekla: differentiation processes in an Icelandic volcano. *Contributions to Mineralogy and Petrology* 112, 20–34. https://doi.org/10.1007/BF00310953

Sigmarsson, O., Bergþórsdóttir, I.A., Devidal, J.-L., Larsen, G., Gannoun, A. (2022) Long or short silicic magma residence time beneath Hekla volcano, Iceland? *Contributions to Mineralogy and Petrology* 177, 13. https://doi.org/10.1007/s00410-021-01883-5

Thirlwall, M.F., Gee, M.A.M., Taylor, R.N., Murton, B.J. (2004) Mantle components in Iceland and adjacent ridges investigated using double-spike Pb isotope ratios. *Geochimica et Cosmochimica Acta* 68, 361–386. https://doi.org/10.1016/S0016-7037(03)00424-1

Thirlwall, M.F., Gee, M.A.M., Lowry, D., Mattey, D.P., Murton, B.J., Taylor, R.N. (2006) Low $\delta^{18}O$ in the Icelandic mantle and its origins: Evidence from Reykjanes Ridge and Icelandic lavas. *Geochimica et Cosmochimica Acta* 70, 993–1019. https://doi.org/10.1016/j.gca.2005.09.008

Tuller-Ross, B., Savage, P.S., Chen, H., Wang, K. (2019) Potassium isotope fractionation during magmatic differentiation of basalt to rhyolite. *Chemical Geology* 525, 37–45. https://doi.org/10.1016/j.chemgeo.2019.07.017

Wang, B., Moynier, F., Jackson, M.G., Huang, F., Hu, X., Halldórsson, S.A., Dai, W., Devos, G. (2023) Rubidium isotopic fractionation during magmatic processes and the composition of the bulk silicate Earth. *Geochimica et Cosmochimica Acta* 354, 38–50. https://doi.org/10.1016/j.gca.2023.05.021

Yang, J., Siebert, C., Barling, J., Savage, P., Liang, Y.-H., Halliday, A.N. (2015) Absence of molybdenum isotope fractionation during magmatic differentiation at Hekla volcano, Iceland. *Geochimica et Cosmochimica Acta* 162, 126–136. https://doi.org/10.1016/j.gca.2015.04.011